Fabrication of CNT/Cu Composite Yarn via Single-Step Electrodeposition

Journal of The Electrochemical Society, 2020 **167** 102509

Fabrication of CNT/Cu Composite Yarn via Single-Step Electrodeposition

Susumu Arai,*,z Ichiro Murakami, Masahiro Shimizu,* and Akimasa Oshigane

Department of Materials Chemistry, Faculty of Engineering, Shinshu University, Wakasato, Nagano 380-8553, Japan

Carbon nanotube (CNT)/Cu composite yarns were formed via a single-step electrodeposition process. A twisted CNT yarn composed of multiwalled CNTs (MWCNTs) was used. Copper was directly electrodeposited onto the CNT yarn under galvanostatic conditions using copper sulfate baths with and without additives. Four additives (polyethylene glycol (PEG), chloride anion (Cl^-), bis(3-sulfopropyl)disulfide (SPS), and Janus green B (JGB)) that are well known as "via-filling additives" were used together. The surface and cross-sectional microstructures of the copper-deposited CNT yarns were analyzed. Copper was electrodeposited only onto the surface of the CNT yarn from the bath without additives, resulting in a copper-coated CNT yarn. By contrast, copper was deposited not only onto the surface but also into the interior of the CNT yarn from the bath with the additives. The amount of copper deposited into the CNT yarn tended to increase with increasing PEG and Cl^- concentrations. The current density also affected the size and location of the deposited copper particles. When the electrodeposition conditions were optimized, copper was relatively homogeneously deposited into the interior of the CNT yarn, resulting in a CNT/Cu composite yarn.
 [DOI: 10.1149/1945-7111/ab9a05]

Manuscript submitted April 28, 2020; revised manuscript received May 21, 2020. Published June 15, 2020.

Carbon nanotube (CNT) yarn,[1–11] which is a one-dimensional macroscopic assembly material composed of CNTs, has attracted intensive attention as a replacement for metallic wires because of its flexibility, high mechanical strength, and low density.[11,12] However, its electrical conductivity still lags behind those of commonly used metallic wire materials such as copper or aluminum.[13] Although individual CNTs themselves exhibit low electrical resistivity (several $\mu\Omega$ cm),[14] CNT yarns exhibit greater electrical resistivity (12–1000 $\mu\Omega$ cm) than individual CNTs.[15] A treatment method of chemical doping followed by annealing has been developed to improve the electrical conductivity of CNT yarns.[16]

Recently, metallization of CNT yarns, especially metallization using copper, has been studied as a method to dramatically improve the electrical conductivity of CNT yarns. Physical vapor deposition of copper onto a CNT yarn by magnetron sputtering and continuous physical treatments such as drawing and rolling have been reported to improve the electrical conductivity of CNT yarns.[17,18] In these previous works, copper was deposited only onto the surface of the CNT yarns, resulting in copper-coated CNT yarns.

Studies on the metallization of CNT yarns by electrodeposition have also been reported.[19–23] In these reports, aqueous copper sulfate baths without additives were mainly used. In most cases, because hydrophobic CNT yarns with a dense structure were used, copper was deposited onto the surface of CNT yarns, with little deposition of copper inside the yarns, resulting in copper-coated CNT yarns.[19,20] When CNT yarns with numerous pores of several hundred nanometers between adjacent CNTs were used, the electrodeposition of copper not only onto the surface but also into the interior of the CNT yarns was achieved, resulting in CNT/Cu composite yarns.[21] Sundaram et al. proposed a two-step electrodeposition method comprising a copper seeding step with an organic copper bath followed by a copper seed growth step with an aqueous copper bath; they achieved homogeneous electrodeposition of copper in the interior of CNT yarns, resulting in CNT/Cu composite yarns.[22,23] In contrast, we have already reported that the electrodeposition of copper inside a free-standing CNT film (i.e., a CNT sheet composed of CNTs) could be achieved using an aqueous copper sulfate bath with additives via a single-step process.[24]

In the present study, the effects of electrodeposition conditions (e.g., additives) on the morphology of copper deposited onto/into a CNT yarn were investigated with the objective of developing a single-step fabrication process for CNT/Cu composite yarns by electrodeposition.

Experimental

Industrial multiwalled CNT (MWCNT) yarns (TPR Co., Ltd.) available as 10 m spools were used. They were single filaments (yarn diameter: ~40 μm) manufactured by continuous twist-spinning of substrate-grown vertical MWCNT arrays (CNT diameter: ~10 nm, array height corresponds to CNT length: 130 μm). The CNT yarn exhibited a neat appearance and good flexibility (Fig. 1a). Surface images of the yarn, as obtained by scanning electron microscopy (SEM), are shown in Fig. 1b (low magnification) and Fig. 1c (high magnification). The yarn had a uniform thickness and a twisted texture (Fig. 1b). Although a few gaps of 100–200 nm diameter were observed on the surface of the CNT yarn (Fig. 1c), the CNT yarn had an overall dense morphology. A dense texture without large gaps in the interior of the CNT yarn was also confirmed by cross-sectional SEM observations (Fig. 1d). These SEM images were collected using the electron microscope described in the next paragraph.

A schematic of the electrodeposition-cell setup is shown in Fig. 2. The CNT yarn was cut and then covered using masking tape with an exposed length of 3 cm. A molybdenum weight covered with masking tape was attached to one end of the masked CNT yarn to apply tension to the CNT yarn during the electrodeposition process. The CNT yarn was then placed in the center of a glass beaker cell, where it was used as the cathode. Four pure copper plates (anode) covered with masking tape so that their exposed surface area was 1.5 cm × 4 cm (6 cm^2) were prepared and were arranged symmetrically at four corners in the glass beaker cell. An aqueous solution composed of 0.85 M $CuSO_4 \cdot 5H_2O$ and 0.55 M H_2SO_4 was used as the base bath. As shown in Table I, polyethylene glycol (PEG) with a mean molecular weight of 2000, chloride ions (Cl^-, as HCl), bis(3-sulfopropyl) disulfide (SPS), and Janus green B (JGB) were added to the base bath as additives (well-known via-filling additives); three additive baths (bath A, bath B, and bath C) were prepared. Bath B contained fivefold greater concentrations of PEG and Cl^- than bath A, and bath C contained twofold greater concentrations of PEG and Cl^- than bath B (Table I). Electrodeposition was performed using an electrochemical measurement system (HZ-7000 Hokuto Denko), where an Ag/AgCl electrode (+0.199 V vs SHE) was adapted to the previously described cell setup, under chronopotentiometry mode at 25 °C and without agitation. In this measurement system, the CNT yarn, the four copper plates, and the Ag/AgCl electrode are the working electrode, the counter electrode, and the reference electrode, respectively. The

*Electrochemical Society Member.
zE-mail: araisun@shinshu-u.ac.jp

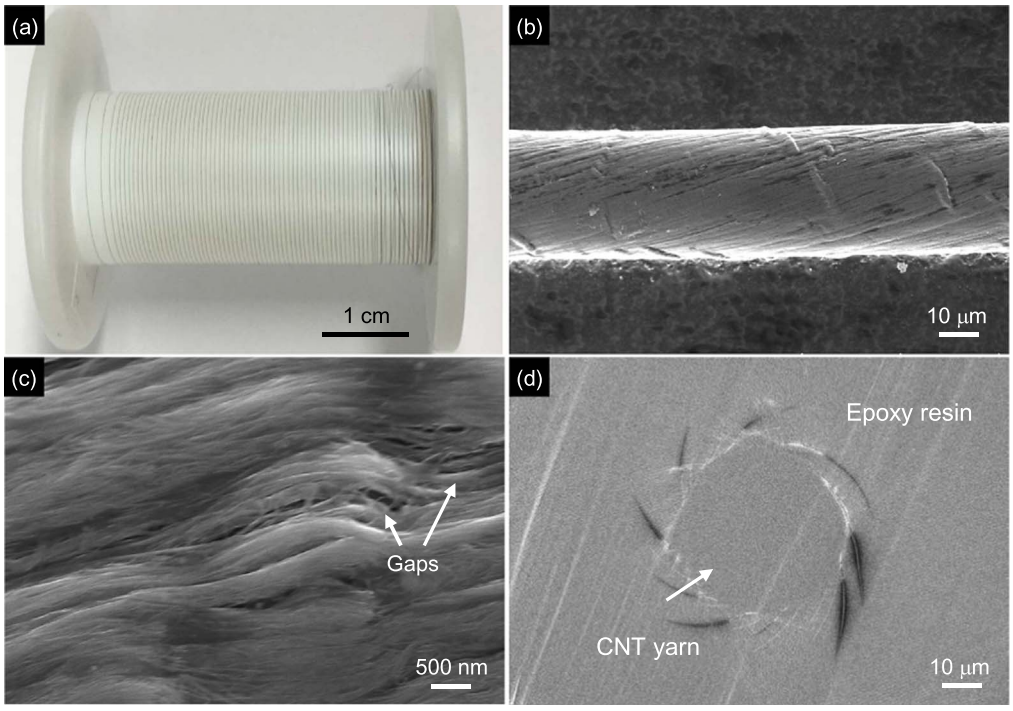

Figure 1. (a) Appearance of a CNT yarn. (b) Surface SEM image of a CNT yarn. (c) High-magnification image of the specimen shown in (b). (d) Cross-sectional SEM image of the CNT yarn.

surface and cross-sectional morphologies of samples were observed using field-emission scanning electron microscopy (FE-SEM; SU 8000 Hitachi High-Tech). Cross-sectional samples were prepared using ion milling equipment (IM 4000 Hitachi High-Tech). Samples were embedded in an epoxy resin before the ion milling process. Elementary mapping analysis of the cross-sectional samples was also conducted by FE-SEM (7000F JEOL) in conjunction with energy-dispersive X-ray spectroscopy.

Results and Discussion

Figure 3 displays the surface morphologies of the CNT yarns after the electrodeposition of copper from various baths with various electrical charges at a current of 0.38 mA. The current of 0.38 mA corresponds to a current density of 10 mA cm^{-2} if the cathode area is assumed to be the surface area of the exposed CNT yarn and the cathode area is assumed to not change during electrodeposition. Panels a–d of Fig. 3 display surface morphologies of the CNT yarns with an electrical charge of 0.11 C from various baths. In the case of the base bath, copper grains with a ~5 μm diameter are observed to be distributed across the surface; however, most of the surface of the CNT yarn was not coated with copper (Fig. 3a). By contrast, the CNT yarns from the additive baths were entirely coated with deposited copper grains with 1–2 μm diameters (Figs. 3b–3d). However, uncoated regions—that is, the exposed surface of the CNT yarn—were also observed on these samples. Panels a′–d′ of Fig. 3 display the surface morphologies of the CNT yarns with copper deposited with an electric charge of 0.58 C from various baths. All of the CNT yarns were perfectly coated with the deposited copper. In the case of the base bath, the CNT yarn was coated with copper grains with a diameter of ~5 μm (Fig. 3a′). By contrast, in the cases of additive baths, the CNT yarns were coated with very small copper grains, resulting in smooth surface morphologies (Figs. 3b′–3d′). Panels a″–d″ of Fig. 3 show the surface morphologies of the CNT yarns with an electric charge of 1.28 C from various baths. Compared with the copper-coated CNT yarns obtained with an electric charge of 0.58 C, those deposited with a charge of 1.28 C exhibited a larger diameter but the same surface morphology.

Figure 4 displays cross-sectional SEM images of the CNT yarns after the electrodeposition of copper from various baths at a current of 0.38 mA. Panels a–d of Fig. 4 display cross-sectional morphologies of the CNT yarns with an electrical charge of 0.11 C from various baths. Copper was electrodeposited only onto the surface of the CNT yarn from the base bath (Fig. 4a). By contrast, copper was deposited not only onto but also into the CNT yarns from the additive baths (Figs. 4b–4d). The amount of deposited copper increased in the order bath A, bath B, bath C, that is, with increasing concentrations of PEG and Cl^-. PEG and Cl^- inhibit copper electrodeposition in a sulfate bath via a synergic effect.[25–36] In addition, copper electrodeposition is also inhibited by the synergic

Table I. Bath compositions.

Reagent	Base Bath	Bath A	Bath B	Bath C
$CuSO_4 \cdot 5H_2O$	0.85 mol dm^{-3}	0.85 mol dm^{-3}	0.85 mol dm^{-3}	0.85 mol dm^{-3}
H_2SO_4	0.55 mol dm^{-3}	0.55 mol dm^{-3}	0.55 mol dm^{-3}	0.55 mol dm^{-3}
PEG2000		100 ppm	500 ppm	1000 ppm
Cl^- (as HCl)		50 ppm	250 ppm	500 ppm
SPS		2 ppm	2 ppm	2 ppm
JGB		2 ppm	2 ppm	2 ppm

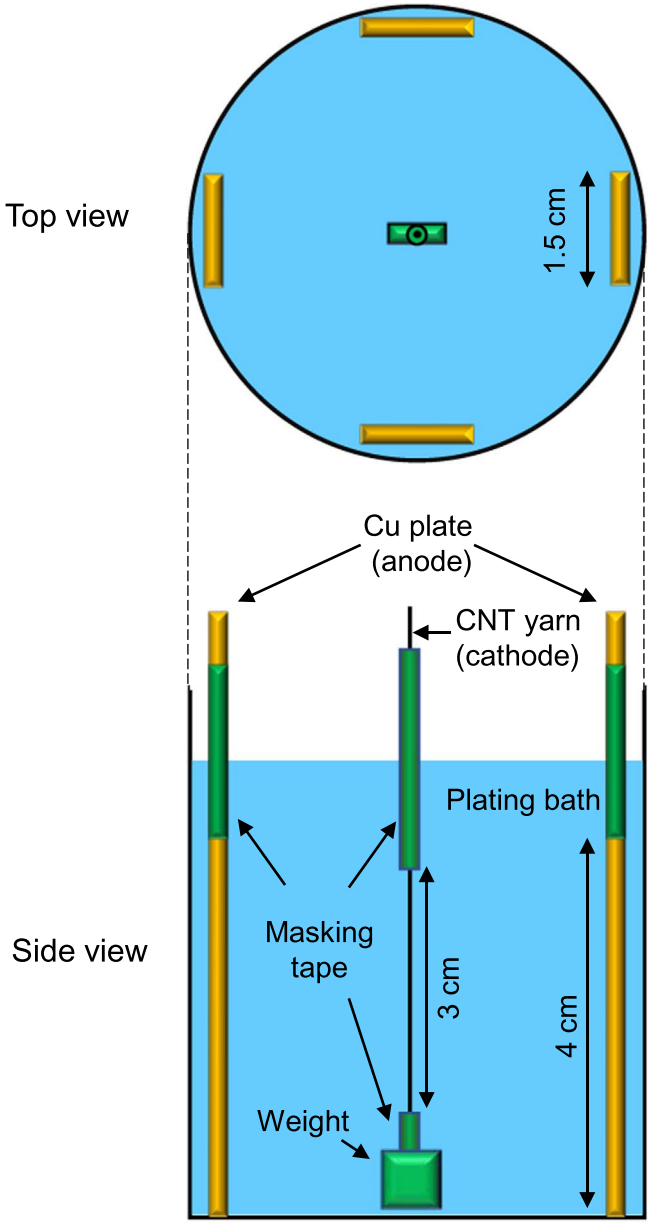

Figure 2. Schematic of the electrolytic cell setup.

effect of PEG and Cl^-, even in the presence of SPS and JGB.[37,38] Therefore, the electrodeposition of copper onto the surface of the CNT yarn should be suppressed by the synergic effect of PEG and Cl^-, resulting in copper deposition both inside the CNT yarn and onto its surface. Increasing the concentrations of PEG and Cl^- further inhibited copper deposition onto the surface of the CNT yarn, resulting in an increase in copper deposition inside the CNT yarn. Panels a′–d′ of Fig. 4 display cross-sectional morphologies of the CNT yarns with copper deposited with an electrical charge of 0.58 C from various baths. Copper was electrodeposited only onto the surface of the CNT yarn from the base bath, and the CNT yarn was perfectly coated with copper (Fig. 4a′; see also Fig. 3a′). By contrast, in cases of additive baths, although copper was deposited inside the CNT yarn, the surface of the yarn was also coated perfectly with deposited copper (Figs. 4b′–4d′; see also Figs. 3b′–3d′). Panels a″–d″ of Fig. 4 display cross-sectional morphologies of the CNT yarns with copper deposited with an electrical charge of 1.28 C from various baths. Electrodeposition of copper inside the CNT yarn did not proceed; copper deposited only onto the previously deposited copper on the surface of the CNT yarns. This result is attributed to the penetration of the baths into the CNT yarns being impeded by the copper film deposited onto the surface of the CNT yarns.

Figure 5 shows the elemental mapping results for the CNT yarns after copper electrodeposition at 0.38 mA with an electric charge of 1.28 C from the base bath and from bath B. In the case of the deposition conducted in the base bath, copper is distributed only on the surface of the CNT yarn, resulting in a copper-coated CNT yarn (Figs. 5a–5c). By contrast, in the case of electrodeposition in bath B, copper was deposited inside the CNT yarn, resulting in a copper-coated CNT yarn with a CNT/Cu composite area inside the yarn (Figs. 5d–5f).

Figure 6 shows the chronopotentiograms corresponding to the electrodeposition of copper onto the CNT yarns at 0.38 mA from various baths. The three vertical dotted lines in this figure denote the

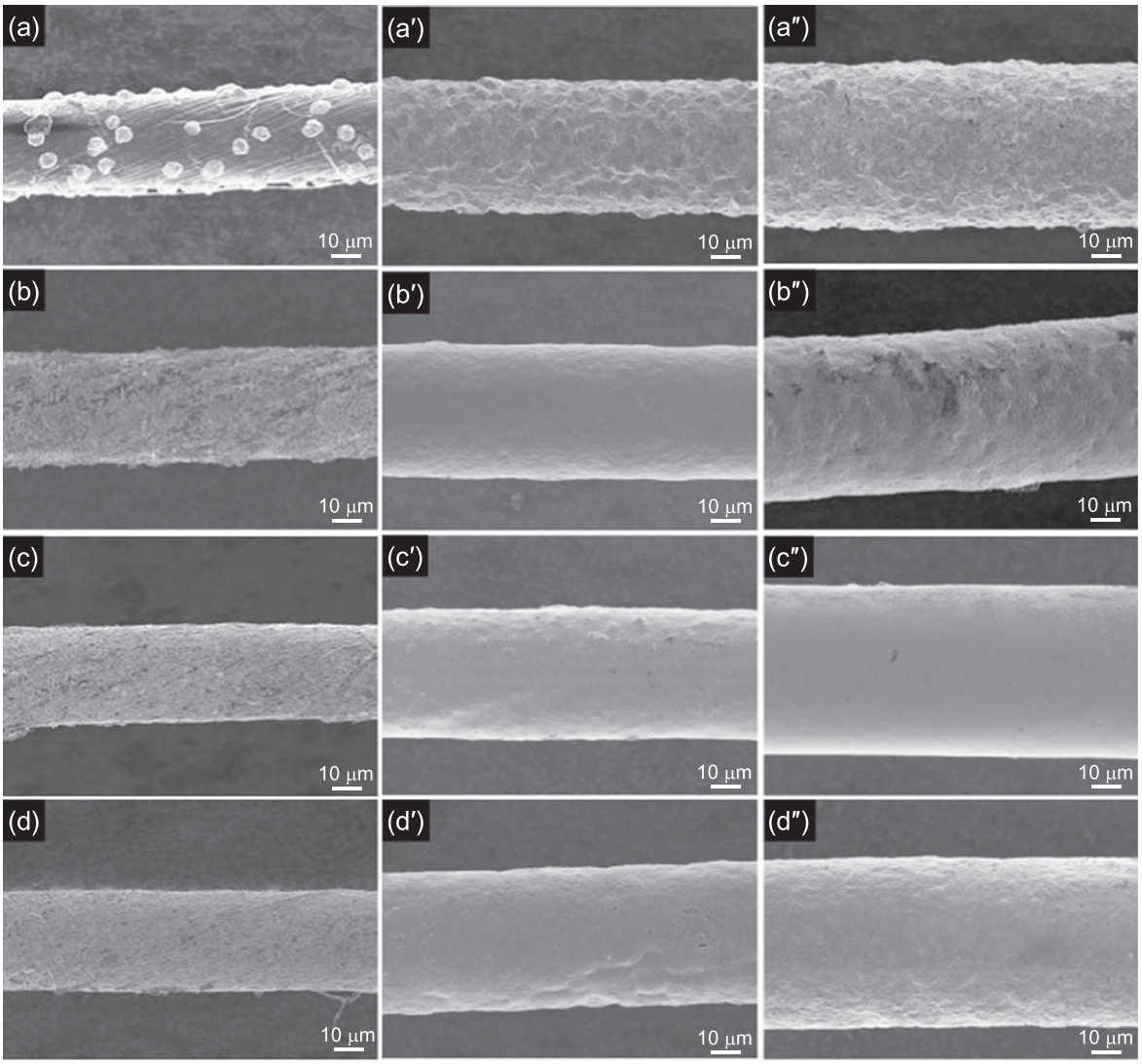

Figure 3. Surface SEM images of copper-deposited CNT yarns with different electrical charges using copper sulfate baths containing different concentration of additives: (a) base bath, 0.11 C, (a′) base bath, 0.58 C, (a″) base bath, 1.28 C, (b) bath A, 0.11 C, (b′) bath A, 0.58 C, (b″) bath A, 1.28 C, (c) bath B, 0.11 C, (c′) bath B, 0.58 C, (c″) bath B, 1.28 C, (d) bath C, 0.11 C, (d′) bath C, 0.58 C, and (d″) bath C, 1.28 C.

times that correspond to electrical charges of 0.11, 0.58, and 1.28 C, respectively. The potential for the base bath (black line) fluctuated until ∼400 s and shifted gradually toward more positive potentials. By contrast, the potentials for the additive baths (bath A: red line, bath B: blue line, and bath C: green line) fluctuated greatly until ∼1200 s and also shifted gradually toward more positive potentials. The potentials corresponding to the additive baths are more negative than that corresponding to the base bath; that is, the overpotentials of the additive baths are larger than that of the base bath. In the case of the base bath, the changing potential until ∼400 s, including 280 s, which corresponds to 0.11 C, is likely attributable to the change of the cathode area on the surface of the CNT yarn (Figs. 3a and 4a). After ∼400 s, including 1530 s (0.58 C) and 3500 s (1.28 C), the surface area of the cathode gradually increased, as shown in Fisg. 3a′, 3a″. This increase should lead to a gradual decrease in the current density (i.e., a gradual decrease in the cathode overpotential), resulting in a gradual shift toward the positive direction. By contrast, in the case of the additive baths, the potential changes until ∼1200 s, which includes 280 s (0.11 C), should be due to the change in the cathode area not only on the surface but also inside the surface of the CNT yarns (Figs. 4b–4d). After ∼1200 s, which includes 1530 s (0.58 C) and 3500 s (1.28 C), the surface area of the cathode increased gradually (Figs. 4b′–4d′, 4b″–4d″), resulting in the observed gradual shift toward more positive potentials, as previously described. The resistance (resistivity) of the CNT yarn cathode likely decreased during copper electrodeposition, and this probably affected the gradual shift toward positive potentials to some extent.

Figure 7 shows cross-sectional SEM images of the CNT yarns with copper deposited from bath B with an electric charge of 0.58 C at various currents (current densities). The amount of copper deposited in the CNT yarn increased with increasing applied current. Meanwhile, the amount of copper deposited onto the surface of the CNT yarn decreased with increasing applied current. In the case of 1.13 mA, copper deposition also occurred at the center of the CNT yarn and the size of the deposited copper grains in the yarn was several hundred nanometers—smaller than the grains of the copper deposited at 0.19 and 0.38 mA (1–2 μm) (panels a and b, respectively, of Fig. 7). Thus, the current density affected the location of copper deposition and the size of the deposited copper particles in the CNT yarn.

Figure 8 displays the elemental mapping analysis results corresponding to Fig. 7c. Although, the CNT yarn is coated with a thin

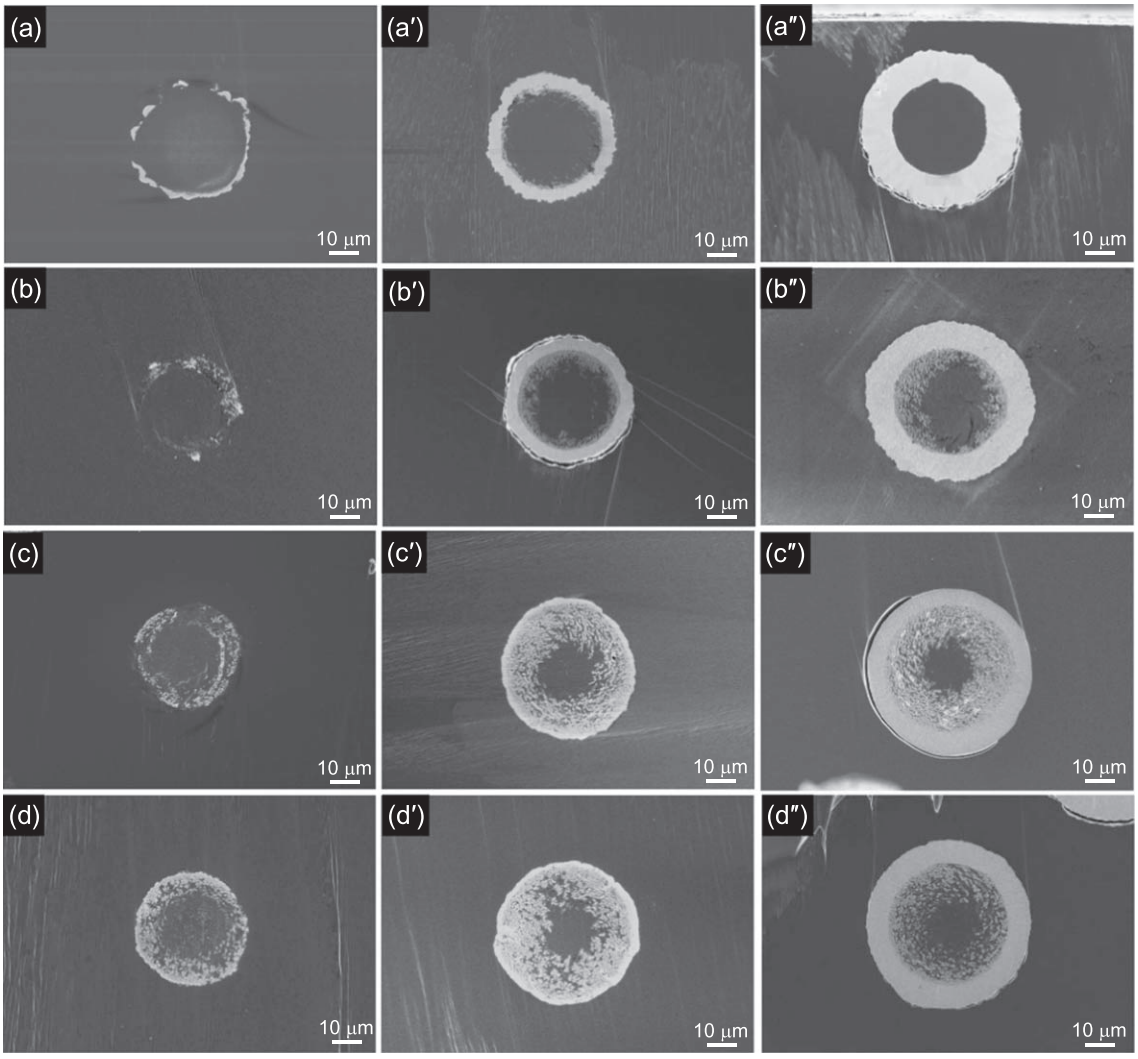

Figure 4. Cross-sectional SEM images of copper-deposited CNT yarns with different electrical charges using copper sulfate baths containing different concentrations of additives: (a) base bath, 0.11 C, (a′) base bath, 0.58 C, (a″) base bath, 1.28 C, (b) bath A, 0.11 C, (b′) bath A, 0.58 C, (b″) bath A, 1.28 C, (c) bath B, 0.11 C, (c′) bath B, 0.58 C, (c″) bath B, 1.28 C, (d) bath C, 0.11 C, (d′) bath C, 0.58 C, and (d″) bath C, 1.28 C.

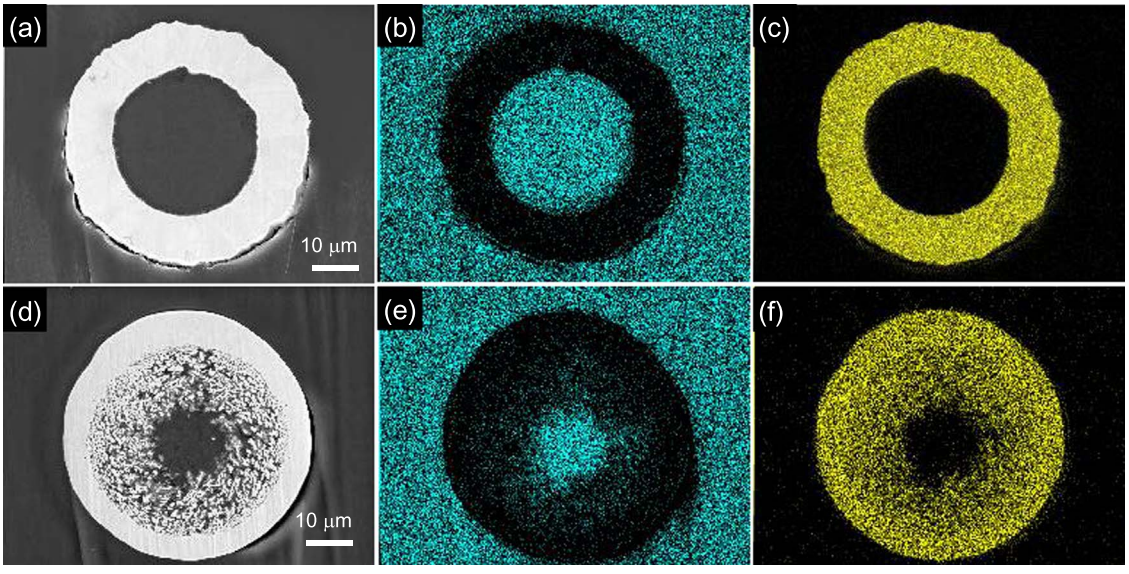

Figure 5. Elemental mapping analysis of cross sections of copper-deposited CNT yarns with an electrical charge of 1.28 C using the base bath and bath B: (a) backscattered electron micrograph for the base bath, (b) carbon distribution in the image shown in (a), and (c) copper distribution in the image shown in (a). (d) Backscattered electron micrograph for bath B. (e) Carbon distribution in the image shown in (d) and (f) copper distribution for bath B.

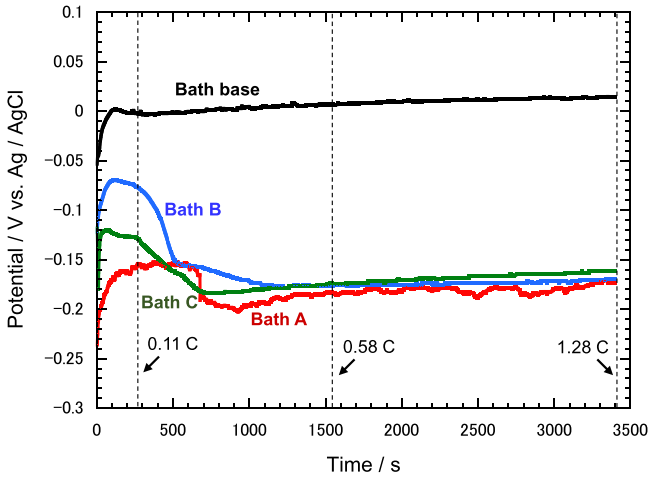

Figure 6. Chronopotentiometry during copper electrodeposition using various plating baths. The current is 0.38 mA.

copper film (∼1 μm) and the copper concentration is lower at the central area, copper is uniformly distributed to some degree across the CNT yarn, almost resulting in CNT/Cu composite yarn.

Figure 9 shows the chronopotentiometry during the electrodeposition of copper on the CNT yarns from bath B at various currents (0.19 mA: green line, 0.38 mA: blue line, and 1.13 mA: red line). The electrical charge is 0.58 C. The cathode potential shifted toward the more negative direction with increasing current (current density); that is, the cathode overpotential increased with increasing current (current density). The difference in cathode potentials between 0.19 mA and 0.38 mA is relatively small, whereas the cathode potential corresponding to 1.13 mA is clearly more negative than those of the other two samples; that is, the current of 1.13 mA resulted in an obviously larger overpotential. This larger overpotential is likely related to the greater amount of copper deposited and smaller size of the deposited copper in the CNT yarn.

Figure 10 depicts schematics of the copper electrodeposition mechanism of the base bath (additive-free bath) and the additive baths. In the case of the additive-free bath, because the surface of the CNT yarn is hydrophobic, the aqueous plating bath does not well wet the CNT yarn. Consequently, copper electrodeposition proceeds only on the surface of the CNT yarn, resulting in a copper-coated CNT yarn (Fig. 10a). By contrast, in the case of the additive bath, which contains PEG, Cl^-, SPS, and JGB, the PEG should act as a surfactant and improve the wetting of the CNT yarn by the bath,[24] resulting in some penetration of the bath into the CNT yarn, especially into the gaps of the CNT yarn (Fig. 1c). During the electrodeposition, PEG and Cl^- should inhibit the electrodeposition of copper onto the copper grains already deposited onto the surface of the CNT yarn via a synergic effect. Consequently, the copper deposition rate inside the CNT yarn increased compared with that on the surface under galvanostatic conditions. The copper deposited inside the CNT yarn increased, widening the gaps and hydrophilizing their interiors, resulting in further penetration of the plating bath into the CNT yarn. Because PEG has a greater molecular weight than the other three additives and is more difficult to diffuse into the gaps, the composition of the plating bath inside the CNT yarn gradually became base bath plus Cl^-, SPS, and JGB, excluding PEG. The Cl^-, SPS, and JGB likely accelerated the electrodeposition of copper into the CNT yarn by a single effect and/or a synergic effect, resulting in a CNT/Cu composite yarn (Fig. 10b).[37–41]

The current density (i.e., the cathode overpotential) should influence the grain size of deposited copper. In the case of the additive bath, when the surface of the CNT yarn is exposed to the bath, copper deposition inside the CNT yarn can continue. However, after the CNT yarn has been perfectly coated with copper, the penetration of the plating bath into the CNT yarn is blocked, resulting in copper deposition only on the surface of the CNT yarn. In summary, both the inhibition of copper deposition on the surface of the CNT yarn and the acceleration of copper deposition into the CNT yarn are important in fabricating CNT/Cu composite yarns.

Thus, one-step fabrication of the CNT/Cu composite yarn can be achieved by electrodeposition using a copper plating bath containing both an inhibitor and an accelerator. The properties of the CNT/Cu

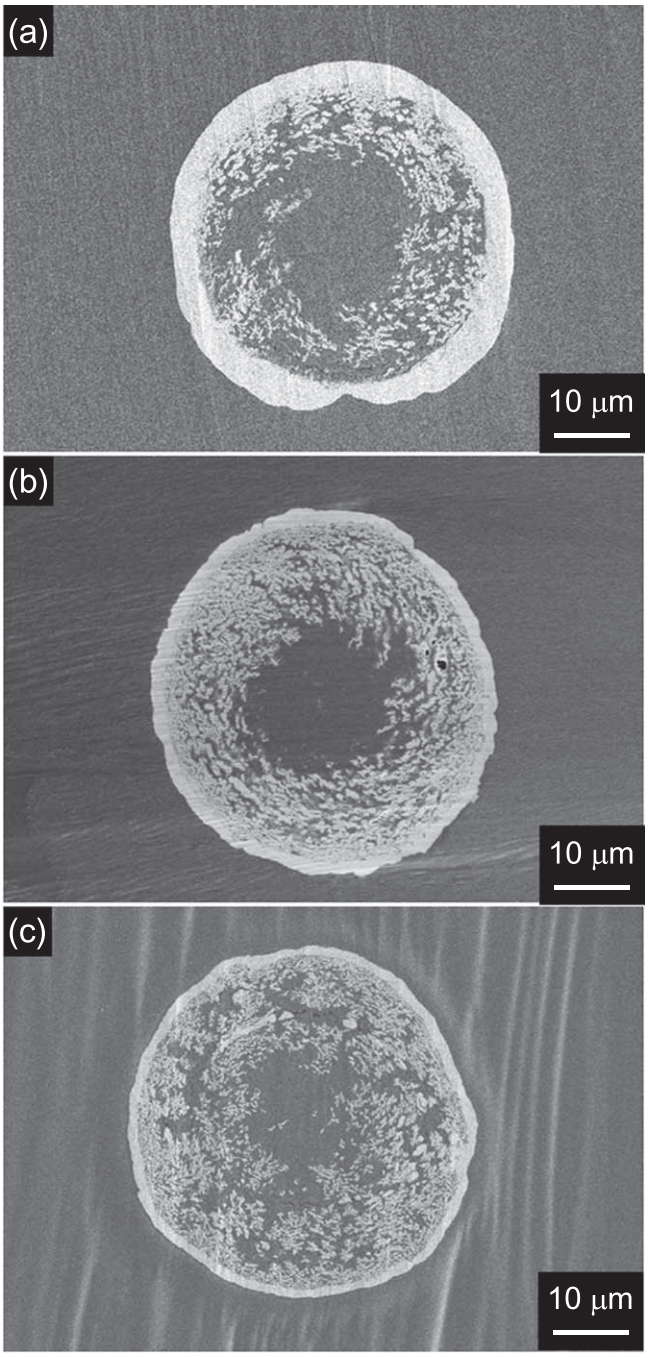

Figure 7. Cross-sectional SEM images of copper-deposited CNT yarns using bath B with an electrical charge of 0.58 C at different currents: (a) 0.19 mA, (b) 0.38 mA, and (c) 1.13 mA.

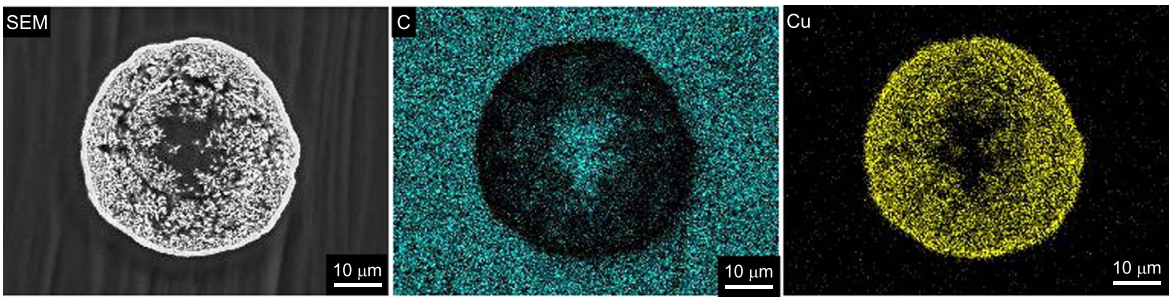

Figure 8. Elemental mapping analysis for the cross section of copper-deposited CNT yarn using the bath B with an electrical charge of 0.58 C at a current of 1.13 mA.

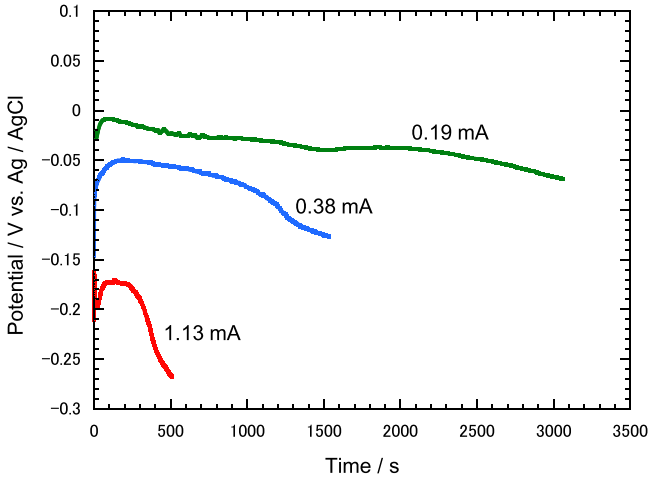

Figure 9. Chronopotentiometry during electrodeposition using bath B at various currents.

composite yarn, such as its electric conductivity, will be evaluated in detail in our future work.

Conclusions

The single-step fabrication of CNT/Cu composite yarns was examined by electrodeposition. The effects of additives (PEG, Cl^-, SPS, and JGB) on the morphology of electrodeposited copper onto/into the CNT yarn were investigated. Copper was electrodeposited only onto the surface of the CNT yarns using a copper sulfate bath without additives, resulting in copper-coated CNT yarns. By contrast, copper deposition occurred not only on but also in the CNT yarns; consequently, a CNT/Cu composite was formed inside the CNT yarn. This composite area was increased through optimization of the electrodeposition conditions such as the current density, resulting in a CNT/Cu composite yarn.

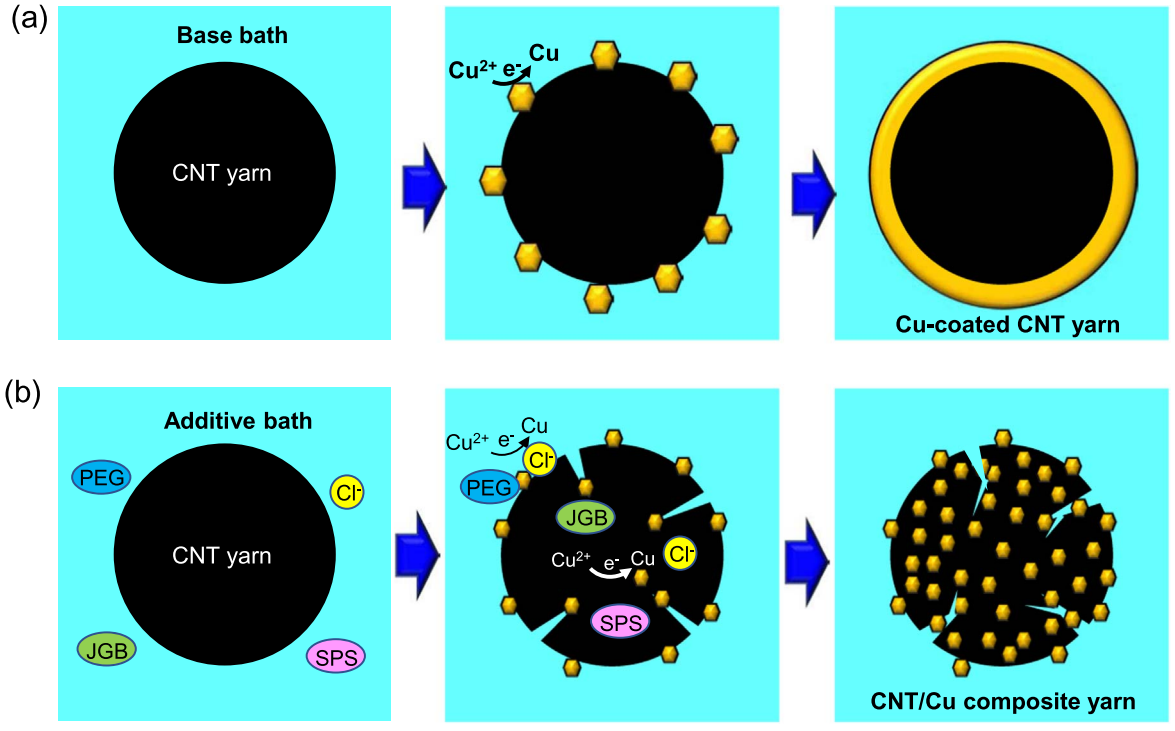

Figure 10. Schematic of the differences in copper deposition morphology of copper deposited from (a) the base bath (additive-free bath) and (b) the additive bath.

Acknowledgments

We thank Junzo Yana of Saitama Industrial Promotion Public Corporation for useful discussions on the science of CNT yarns. We also thank the members of nanocarbon study group (CNT wire) of Saitama prefecture for useful discussions on the application of CNT yarns.

ORCID

Susumu Arai https://orcid.org/0000-0002-4915-0398
Masahiro Shimizu https://orcid.org/0000-0003-1084-7486

References

1. K. Jiang, Q. Li, and S. Fan, *Nature*, **419**, 801 (2002).
2. M. Zhang, K. R. Atkinson, and R. H. Baughman, *Science*, **306**, 1358 (2004).
3. K. Liu, F. Zhu, L. Liu, Y. Sun, S. Fun, and K. Jiang, *Nanoscale*, **4**, 3389 (2012).
4. L. Qiu, X. Wang, D. Tang, X. Zheng, P. M. Norris, D. Wen, J. Zhao, X. Zhang, and Q. Li, *Carbon*, **105**, 248 (2016).
5. Y. L. Li, I. A. Kinloch, and A. H. Windle, *Science*, **304**, 276 (2004).
6. J. N. Wang, X. G. Luo, T. Wu, and Y. Chen, *Nat. Commun.*, **5**, 3848 (2014).
7. T. Q. Tran, Z. Fan, A. Mikhalchan, P. Liu, and H. M. Duong, *ACS Appl. Mater. Interfaces*, **8**, 7948 (2016).
8. Y. Shang, Y. Wang, S. Li, C. Hua, and M. Zou, *Carbon*, **119**, 47 (2017).
9. J. Choi, Y. Jung, S. J. Yang, J. Y. Oh, J. Oh, K. Jo, J. G. Son, S. E. Moon, C. R. Park, and H. Kim, *ACS Nano*, **11**, 7608 (2017).
10. N. Bahabtu et al., *Science*, **339**, 182 (2013).
11. R. J. Headrick, D. E. Tsentalovich, J. Berdegue, E. A. Bengio, L. Liberman, O. Kleinerman, M. S. Lucas, Y. Talmon, and M. Pasquali, *Adv. Mater.*, **30**, 1704482 (2018).
12. T. Q. Tran, Z. Fan, P. Liu, S. M. Myint, and H. M. Duong, *Carbon*, **99**, 407 (2016).
13. A. Lekawa-Raus, L. Kurzepa, X. Peng, and K. Koziol, *Carbon*, **68**, 597 (2014).
14. T. M. Ebbesen, H. J. Lezec, H. Hiura, J. W. Bennett, H. F. Ghaemi, and T. Thio, *Nature*, **382**, 54 (1996).
15. Y. Dini, J. Faure-Vincent, and J. Dijon, *Carbon*, **144**, 301 (2019).
16. Y. Dini, D. Rouchon, J. Faure-Vincent, and J. Dijon, *Carbon*, **156**, 38 (2020).
17. B. Han, E. Guo, X. Xue, Z. Zhao, L. Luo, H. Qu, T. Niu, Y. Xu, and H. Hou, *Carbon*, **123**, 593 (2017).
18. B. Han, E. Guo, X. Xue, Z. Zhao, T. Li, Y. Xu, L. Luo, and H. Hou, *Appl. Surf. Sci.*, **441**, 984 (2018).
19. L. K. Randeniya, A. Bendavid, P. J. Martin, and C. D. Tran, *Small*, **6**, 1806 (2010).
20. G. Xu, J. Zhao, S. Li, X. Zhang, Z. Yong, and Q. Li, *Nanoscale*, **3**, 4215 (2011).
21. P. Hannula, A. Peltonen, J. Aromaa, D. Janas, M. Lundstrom, B. P. Wilson, K. Koziol, and O. Forsen, *Carbon*, **107**, 281 (2016).
22. R. Sundaram, T. Yamada, K. Hata, and A. Sekiguchi, *Sci. Rep.*, **7**, 9267 (2017).
23. R. Sundaram, T. Yamada, K. Hata, and A. Sekiguchi, *Mater. Today Commun.*, **13**, 119 (2017).
24. S. Arai, K. Kirihata, M. Shimizu, M. Ueda, A. Katada, and M. Uejima, *J. Electrochem. Soc.*, **164**, D922 (2017).
25. M. R. H. Hill and G. T. Rogers, *J. Electroanal. Chem.*, **86**, 179 (1978).
26. M. Yokoi, S. Konishi, and T. Hayashi, *Denki Kagaku*, **52**, 218 (1984).
27. J. D. Reid and A. P. David, *Plating Surf. Fin.*, **74**, 66 (1987).
28. M. Goodenough and K. J. Whitelaw, *Trans. Inst. Metal Fin.*, **67**, 57 (1989).
29. J. P. Healy, D. Pletcher, and M. Goodenough, *J. Electroanal. Chem.*, **338**, 155 (1992).
30. Z. V. Feng, X. Li, and A. A. Gewirth, *J. Phys. Chem. B*, **107**, 9415 (2003).
31. K. R. Hebert, *J. Electrochem. Soc.*, **152**, C283 (2005).
32. M. E. H. Garrido and M. D. Pritzker, *J. Electrochem. Soc.*, **155**, D332 (2008).
33. H. M. Chen, S. J. Parulekar, and A. Zdunek, *J. Electrochem. Soc.*, **155**, D341 (2008).
34. M. E. H. Garrido and M. D. Pritzker, *J. Electrochem. Soc.*, **156**, D36 (2009).
35. M. E. H. Garrido and M. D. Pritzker, *J. Electrochem. Soc.*, **156**, D175 (2009).
36. A. Chrzanowska and R. Mroczka, *Electrochim. Acta*, **78**, 316 (2012).
37. J. J. Kelly, C. Tian, and A. C. West, *J. Electrochem. Soc.*, **146**, 2540 (1999).
38. P. Taephaisitphongse, Y. Cao, and A. C. West, *J. Electrochem. Soc.*, **148**, C492 (2001).
39. M. Tan and J. N. Harb, *J. Electrochem. Soc.*, **150**, C420 (2003).
40. K. Kondo, T. Matsumoto, and K. Watanabe, *J. Electrochem. Soc.*, **151**, C250 (2004).
41. M. Tan, C. Guymon, D. R. Wheeler, and J. N. Harb, *J. Electrochem. Soc.*, **154**, D78 (2007).